American Mineralogist, Volume 93, pages 1429–1436, 2008

Synthetic hypersilicic Cl-bearing mica in the phlogopite-celadonite join: A multimethodical characterization of the missing link between di- and tri-octahedral micas at high pressures

SABRINA NAZZARENI,[1,*] PAOLA COMODI,[1] LUCA BINDI,[2] OLEG G. SAFONOV,[3] YURIY A. LITVIN,[3] AND LEONID L. PERCHUK[3,4]

[1]Department of Earth Sciences, University of Perugia, Perugia, Italy
[2]Museo di Storia Naturale, Sezione di Mineralogia, Università di Firenze, Via La Pira 4, I-50121, Firenze, Italy
[3]Institute of Experimental Mineralogy, Chernogolovka, Moscow, Russia
[4]Department of Petrology, Moscow State University, Moscow, Russia

ABSTRACT

A hypersilicic Cl-bearing mica was synthesized at 4 GPa and 1200–1250 °C, close to the solidus of the join diopside-jadeite-KCl, in association with diopside-jadeite pyroxene, K-rich aluminosilicate glass and/or sanidine and (K,Na)Cl. The mica shows a negative correlation between tetrahedral Si and octahedral (Al + Mg), suggesting an Al-celadonitic substitution (Si + ^{VI}Al + $^{VI}\square$ = ^{IV}Al + ^{VI}Mg) and a chemical formula: $K_{1.01}(Mg_{2.45}Al_{0.19}\square_{0.35})_{\Sigma=3}(Si_{3.52}Al_{0.48})_{\Sigma=4}O_{10}[(OH,O)_{1.66}Cl_{0.34})]_{\Sigma=2}$. The presence of hydroxyl was confirmed by OH stretching modes at 3734 and 3606 cm^{-1} in the Raman spectra. Single-crystal X-ray diffraction data provide the unit-cell parameters (space group *C*2/*m*, 1*M* polytype): a = 5.299(4), b = 9.167(3), c = 10.226(3) Å, β = 100.06(4)°, V = 489.1(4) $Å^3$. The structure refinement shows the presence of vacancies on the octahedral sites (15% for M1 and 6.5% for M2). Chlorine occupies a position about 0.5 Å from O4 with partial occupancy (0.39 apfu). Crystal-chemical mechanisms seem to govern chlorine incorporation in mica, since a large A site is necessary to locate the anion in the structure. A large A site results when the six-tetrahedra ring is hexagonal and the tetrahedral rotation angle α is 0°. Such a geometry is achieved either by increasing the annite component in biotite or by increasing the hypersilicic character of phlogopite through the Al-celadonite substitution. The present Si-rich mica shows a partial dioctahedral character due to the Al-celadonite substitution, which lowers the α angle and expands its stability field at high pressure.

High a_{K_2O} conditions, like in potassium-rich brine or potassic carbonatitic melts, increase the Al-celadonite component in the phlogopite solid solution, explaining the association of Si-rich micas with inclusions of potassic liquids in kimberlitic diamonds.

Keywords: Phlogopite, Al-celadonite, chlorine, high pressure, solid solution, kimberlites, inclusions in diamonds

INTRODUCTION

The role of micas in mantle-related processes is hard to overestimate. Being hosts of potassium and water, micas are able to carry chlorine and fluorine, as well as geochemically important trace elements, such as Ba, Rb, Cs, Pb, and Li. Both dioctahedral (phengite) and trioctahedral (phlogopite) micas are stable at upper-mantle pressures. However, there is a strong difference between the occurrences of both groups of micas. Phengite has never been observed in mantle xenoliths, nor has it been found as inclusions in kimberlitic diamonds. Probably, the main reason for the absence of phengite in mantle xenoliths and diamonds is its relatively low temperature of stability, just up to 1000–1050 °C (Schmidt and Poli 1998; Domanik and Holloway 2000), which is compatible with "cold" high-pressure environments of subducted oceanic slabs. Phengite, indeed, is a leading hydrous phase in eclogites related to HP-UHP metamorphism. In contrast, phlogopite is stable up to 1400 °C within a wide pressure interval (e.g., Yoder and Kushiro 1969; Trønnes 2002), while extensive isomorphic substitutions (Ti, F) substantially expand its stability (e.g., Harlow 2002). Therefore, phlogopite is a common mineral in mantle xenoliths, and it occurs as inclusions in kimberlitic diamonds worldwide. Phlogopite inclusions in diamonds are associated both with eclogitic (Prinz et al. 1975; Gurney et al. 1979; Sobolev et al. 1997, 1998; Leost et al. 2003) and peridotitic (Sobolev et al. 1997; Bulanova et al. 1993) assemblages. Inclusions of phlogopite of uncertain assemblages are known in diamonds as well (Giardini et al. 1974; Guthrie et al. 1991; Walmsley and Lang 1992).

In most cases, phlogopite from mantle xenoliths and diamonds is regarded to be the product of either the final stages of magma evolution or interaction of upper mantle rocks with alkali and volatile-rich fluids or melts. An assemblage of "peridotitic" phlogopite with inclusions of alkali Cl-rich fluids was recently documented in cloudy diamonds from the Koffiefontein pipe, Republic of South Africa (Izraeli et al. 2004). Eclogitic assem-

* E-mail: sabrina.nazzareni@unipg.it

blages in the Koffiefontein fluid-bearing diamonds carry mica, as well. However, this mica shows an unique composition that has never been described in nature till now. In contrast to "normal" phlogopite, this mica contains 6.65–6.73 apfu of Si with low Al (1.5–1.6 apfu) per 22 O. Similar mica with much higher Si content (up to 7.65 apfu) and Al content of 1.0–1.5 apfu is associated with Cl-bearing carbonate-silicate melt in diamond from the Diavik mine, Canada (Klein-BenDavid et al. 2006). In micas from both these occurrences, the Si content shows distinct negative correlation with total occupancy of the octahedral site, suggesting vacancies at this site and the isomorphism $Al^{IV} + (M^{2+} + M^{3+})^{VI} \leftrightarrow 2Si^{IV} + \square^{VI}$ (where M = Mg, Fe, Al, and Ti, are cations in the octahedral sites of the mica structure). Thus, these micas are solid solutions along the Al-celadonite, $KMgAlSi_4O_{10}(OH)_2$, and the complex Ti-bearing phlogopite join. This suggestion is also supported by IR spectra, which show bands of both Al-celadonite and phlogopite (Klein-BenDavid et al. 2006). Micas from both localities differ in Ti content. Moreover, Si-rich micas from the Koffiefontein diamonds contain 4–6 wt% of Cl and the IR spectra do not indicate the presence of hydroxyl (Izraeli et al. 2004). In contrast, micas from the Diavik diamond contain just 0.2–0.4 wt% of Cl (Klein-BenDavid et al. 2006).

Taking into account the close association of the Si-rich micas with both inclusions of alkali-rich fluids and crystalline phases, Izraeli et al. (2004) and Klein-BenDavid et al. (2006) concluded that micas were formed syngenetically with diamonds via fluid interaction with mantle rocks or direct precipitation from a supercritical fluid during cooling. Higher Si and Ti contents in the Cl-poor micas from the Diavik diamonds could be explained by their equilibrium with Ti-enriched carbonate-silicate melt (Klein-BenDavid et al. 2006), while higher Cl and lower Ti contents of micas from the Koffiefontein diamonds could correspond to equilibrium with omphacite and the chloride-carbonate liquid.

Silicon-rich micas linking dioctahedral and trioctahedral end-members are well known from experimental studies. Seifert and Schreyer (1965) first synthesized the $KMg_{2.5}[Si_4O_{10}](OH)_2$ end-member and its solid solution with phlogopite at 0.1 GPa and 620 °C. Franz and Althaus (1974) produced the Na-analog of this mica at 0.1–0.5 GPa and 500–600 °C, while Toraya et al. (1976; 1978) synthesized its F-rich analog from a melt at room pressure and 1100 °C. Silicon-rich, Cl-bearing micas intermediate between phlogopite and $KMg_{2.5}[Si_4O_{10}](OH)_2$ were found in products of experiments on alkali exchange between phlogopite and (K,Rb,Cs)Cl solutions at 0.2–4.0 GPa (Melzer and Wunder 2001; Harlov and Melzer 2002). Silicon-rich, F-rich micas, whose composition is close to the phlogopite-Al-celadonite join, were produced by Foley et al. (1986) in the system $KAlSiO_4$-Mg_2SiO_4-SiO_2-F at 2.8 GPa. However, pure OH-bearing and Cl-bearing intermediate mica within the Al-celadonite-phlogopite join have not been synthesized so far.

In the present paper, we first report the synthesis and crystal chemistry of Cl-rich mica characterized by the substitution $Al^{IV} + (M^{2+}+M^{3+})^{VI} \leftrightarrow 2Si^{IV} + \square^{VI}$. This substitution vector links trioctahedral to dioctahedral micas and confirms the possibility of a solid solution between phlogopite and Al-celadonite at high pressure postulated by Seifert (1968). In the paper, we discuss the role of pressure and chlorine content in the formation of this solid solution.

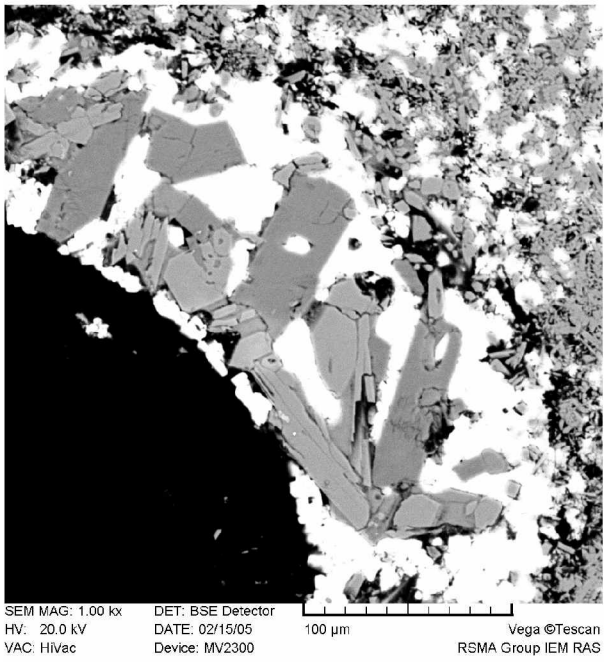

FIGURE 1. BSE images of idiomorphic mica crystals, coexisting with diopside-jadeite clinopyroxene produced in the run 1252 (P = 4 GPa, T = 1250 °C). CamScan electronic microscope.

EXPERIMENTAL METHODS

Synthesis

The Cl-bearing, Si-rich mica was observed as an accessory phase in the run products in the system $CaMgSi_2O_6$-$NaAlSi_2O_6$-KCl at 4 GPa, 1200 and 1250 °C, and 180 min of duration (Safonov, unpublished data). Mixtures of stoichiometric gels $CaMgSi_2O_6$ and $NaAlSi_2O_6$ with 50 mol% of crystalline KCl were used for these experiments. The runs were performed with the high-pressure toroidal "anvil-with-hole" apparatus, which is a modification of the Bridgman-type anvil assembly. Technical details and references can be found in Safonov et al. (2003, 2007).

The formation of the Si-rich mica is related to presence of water in the starting mixtures due to the strong hydroscopic character of KCl. In the run products, mica coexists with diopside-jadeite clinopyroxene and (K,Na)Cl aggregates, as well as with ~10 vol% of Si-rich alkalic aluminosilicate glass and/or sanidine. The Si-rich micas form euhedral flakes of 50–200 µm in size enclosed either in a pyroxene-chloride matrix or in coarse-grained chloride aggregates, which are attached to the walls of capsules (Fig. 1). One crystal of the most Si-rich, Cl-bearing mica was hand-picked under microscope from the run 1252 and used for the X-ray diffraction study and detailed electron microprobe analysis.

X-ray data collection and structural refinement

The X-ray analysis was performed by means of an Oxford Xcalibur single crystal diffractometer equipped with both CCD (Sapphire) and point detectors using Mo$K\alpha$ radiation. Experimental and refinement details are given in Table 1. The collected data, after Lorentz, polarization, and empirical absorption corrections using the SADABS package (Sheldrick 1996), gave a discrepancy factor among symmetry related reflections of R_{int} = 6.08%.

The crystal structure refinement was performed in the space group $C2/m$, starting from the atomic coordinates of phlogopite (Comodi et al. 2004), using the program SHELXL-97 (Sheldrick 1997). At the beginning, an isotropic refinement with neutral scattering curves for K, Mg, Al, Si, O, and Cl (taken from *International Tables for X-ray Crystallography*, vol. IV, Ibers and Hamilton 1974) was undertaken. To account for some residuals in the difference Fourier synthesis (possibly resulted from a shift of atoms by $\pm b/3$ from the basic structure), we added two different scale factors for the reflections with $k \neq 3n$. In fact, to eliminate the spurious peak Oberti et al. (1993) suggested a separate rescaling of reflections with $k \neq 3n$,

TABLE 1. Crystallographic data for the selected Cl-bearing, Si-rich mica crystal

Crystal data	
Temperature (K)	298
Chemical formula	$K_2(Mg,Al)_{5.44}(Si,Al)_{8.00}O_{20}(OH,Cl)_4$
Space group	*C*2/*m*
Cell parameters:	
a (Å)	5.299(4)
b (Å)	9.167(3)
c (Å)	10.226(3)
β (°)	100.06(4)
V (Å^3), *Z* = 2	489.1(4)
Crystal color	transparent
Crystal shape	block
Crytal size (mm)	0.138 × 0.083 × 0.014
Data collection	
Temperature (K)	298 K
Diffractometer	Oxford Diffraction Xcalibur 2
Radiation	Mo*K*-$L_{2,3}$ (0.71073 Å)
Monochromator	oriented graphite (002)
Scan mode	ω
$2\theta_{max}$ (°)	59.2
hkl range	$-7 \le h \le 6$
	$-12 \le k \le 12$
	$-13 \le l \le 13$
No. of reflections	4013
No. of frames	1096
Exposure time (s)	120
Frame width (°)	0.90
Data reduction	
Absorp. correction	SADABS
No. of ind. refl.	4002
Criterion for obs.	$F_o > 4\sigma(F_o)$
No. of observed refl.	1916
R_{int}	0.0608
Refinement	
Ref. coefficient	*F*^{2}
No. of refl. in ref.	4002
No. of refined par.	45
Scale factor for $k \neq 3n$	1.0271
Scale factor for $k = 3n$	0.6476
R_{obs}/R_{all}	0.0439/0.1116
Diff. Fourier (e$^-$/Å^3)	[–0.49, 0.69]

which, being affected by streaking, are systematically underestimated.

In the tetrahedral site the occupancies of Si and Al were constrained from the chemical analysis (12.250 and 1.625 e$^-$, respectively). After the A, M1, and M2 site occupancies were refined (i.e., 19, 10.22, and 11.22 e$^-$, respectively), the obtained values were fixed and the inspection of the difference Fourier map revealed a large peak close to the O4 site. This peak was tentatively assigned as a position partially occupied by Cl. In fact, the O4 site splits into two sub-sites, one of which is occupied by O and the other by Cl. Successive least squares cycles were run by fixing, alternately, the site-occupancy factor and the isotropic displacement parameter. Final occupancy factor for the Cl position was about 20% (i.e., 3.34 e$^-$), and the corresponding occupancy of the O4 position was 80% (i.e., 6.43 e$^-$). Subsequently, the Cl- and O4-site occupancies were fixed and an anisotropic model for the metals was refined. Convergence was achieved quickly to $R = 4.39\%$ for 1916 observed reflections [$F_o > 4\sigma(F_o)$]. At this stage, one peak at 0.95 Å from O4 was also located and assigned as a hydrogen atom. An attempt to refine the H position, however, was unsuccessful. The crystal structure refinement conducted with ionized scattering curves yielded similar results. Thus, only the results from the neutral scattering curves are presented here. Fractional atomic coordinates and anisotropic-displacement parameters are shown in Table 2. Table 3 lists the observed and calculated structure factors.[1]

Chemical composition

Preliminary examination of run products and phase compositions was performed with the CamScan MV2300 (VEGA TS 5130MM) electron microscope equipped with a Link INCA Energy EDS electron microprobe. Detailed microprobe analyses of the mica crystal from run 1252 selected for the X-ray single-crystal study were performed with a JEOL-JXA 8600 microprobe using 15 kV accelerating potential and 10 nA beam current. For the WDS analyses, the following lines were used: Si*K*α, Al*K*α, Mg*K*α, K*K*α, and Cl*K*α. The estimated analytical precision is ±0.90 for SiO_2, ±0.45 for MgO, ±0.35 for K_2O, ±0.25 for Al_2O_3 and ±0.05 for Cl. The crystal fragment was found to be homogeneous within the analytical uncertainty.

Raman spectroscopy

Unoriented Raman spectra on two different sample orientations were collected in the 300–4700 cm^{-1} frequency region, with 30 s counting times and 6 accumulations. The 518 nm laser beam was focused to 5 μm with a 5.4 mW power. In the high frequency region two bands at 3606 and 3734 cm^{-1} were detected. The former is assigned to the V-type OH stretching mode, whereas the latter, to the N-type OH stretching mode for Raman and IR spectra (Robert and Kodama 1988). Both frequencies are close to the values reported for the tetrasilicic mica by Robert and Kodama (1988) who ascribed these bands to different ordering of the neighboring octahedral sites. The N-type OH (at 3735 cm^{-1}) is bonded to 3Mg, whereas the V-type (3595 cm^{-1}) to 2Mg +□.

RESULTS

Crystal chemistry of the Cl-bearing, Si-rich mica

Chemical composition of the mica is reported in Table 4, while geometrical parameters, bond distances, and polyhedral volumes are shown in Table 5. The mean number of electrons calculated for the site populations obtained on the basis of the chemical data (10.64 e$^-$ for <M1 + M2>) are in close agreement with those from the site-occupancy refinement (10.72 e$^-$ for <M1 + M2>). The mean number of electrons for the Cl split-position (3.34 e$^-$) matches fairly the value obtained from the chemical composition (2.86 e$^-$). Since OH bands were detected with Raman spectroscopy, the chemical formula based on 11 O atoms resulted:

[1] Deposit item AM-08-032, Table 3 (CIF). Deposit items are available two ways: For a paper copy contact the Business Office of the Mineralogical Society of America (see inside front cover of recent issue) for price information. For an electronic copy visit the MSA web site at http://www.minsocam.org, go to the American Mineralogist Contents, find the table of contents for the specific volume/issue wanted, and then click on the deposit link there.

TABLE 2. Fractional coordinates, site occupancies (in electrons per formula unit), and anisotropic displacement parameters of atoms for Cl-bearing, Si-rich mica

	x/a	*y/b*	*z/c*	sof	U_{11}	U_{22}	U_{33}	U_{12}	U_{13}	U_{23}	U_{eq}
K	0	0	0	19.00(8)	0.0370(9)	0.0363(6)	0.0484(7)	0	0.0087(6)	0	0.0404(4)
Si	0.5762(1)	0.1670(1)	0.2287(1)	12.25	0.0102(4)	0.0069(2)	0.0138(2)	–0.0001(3)	0.0018(2)	–0.0007(3)	0.0103(1)
Al	0.5762(1)	0.1670(1)	0.2287(1)	1.625	0.0102(4)	0.0069(2)	0.0138(2)	–0.0001(3)	0.0018(2)	–0.0007(3)	0.0103(1)
M1	0	½	½	10.22(4)	0.008(1)	0.0055(6)	0.0103(7)	0	0.0019(7)	0	0.0080(4)
M2	0	0.8320(1)	½	11.22(3)	0.0164(7)	0.0102(4)	0.0175(5)	0	0.0048(5)	0	0.0145(3)
O1	0.8119(3)	0.2435(1)	0.1678(1)								0.0188(3)
O2	0.5428(4)	0	0.1685(2)								0.0166(4)
O3	0.6301(3)	0.1674(1)	0.3893(1)								0.0105(3)
O4	0.1328(6)	0	0.4002(3)	6.43(2)							0.0137(6)
Cl	0.118(1)	0	0.3496(6)	3.34(6)							0.048(2)

TABLE 4. Electron-microprobe data for the selected Cl-bearing, Si-rich mica crystal

	1	2	3	4	5	6	7	mean
SiO_2	52.99	53.02	52.85	53.15	53.08	52.89	53.20	53.03
Al_2O_3	8.70	8.68	8.75	8.62	8.60	8.75	8.59	8.67
MgO	24.74	24.76	24.80	24.82	24.84	24.79	24.81	24.79
K_2O	11.89	11.91	11.88	11.91	11.89	11.86	11.92	11.89
Cl	1.46	1.49	1.50	1.51	1.48	1.52	1.53	1.50
Total	99.78	99.86	99.78	100.01	99.89	99.81	100.05	99.88
O=Cl	0.33	0.34	0.34	0.34	0.34	0.34	0.35	0.34
Total	99.45	99.52	99.44	99.67	99.55	99.47	99.70	99.54
Si	7.032	7.033	7.017	7.040	7.037	7.021	7.045	7.032
Al	1.360	1.357	1.369	1.345	1.343	1.369	1.340	1.355
Mg	4.890	4.892	4.905	4.897	4.905	4.902	4.894	4.898
K	2.012	2.015	2.012	2.012	2.010	2.008	2.013	2.012
Cl	0.328	0.335	0.337	0.339	0.332	0.342	0.343	0.337
Al^{IV}	0.968	0.967	0.983	0.960	0.963	0.979	0.955	0.968
Al^{VI}	0.392	0.389	0.386	0.385	0.381	0.389	0.385	0.387
Al^{VI}+Mg	5.282	5.282	5.291	5.282	5.286	5.291	5.279	5.285

Note: Chemical formulae calculated on the basis of 22 O atoms.

TABLE 5. Bond distances and geometrical parameters for Cl-bearing, Si-rich mica

K-O2	3.084 (3)	T-O3	1.617 (1)	M1-O4	2.033 (3)	M2-O3	2.075 (2)
K-O1	3.085 (2)	T-O1	1.647 (2)	M1-O3	2.094 (1)	M2-O4	2.040 (2)
K-O2	3.209 (3)	T-O1	1.648 (2)	M1-Cl	2.319 (7)	M2-O3	2.085 (2)
K-O1	3.196 (2)	T-O2	1.649 (2)	<M1-O>	2.064	M2-Cl	2.337 (5)
$K\text{-}O_{outer}$	3.203	<T-O>	1.640	<M1-(O-Cl)>	2.074	<M2-O>	2.060
$K\text{-}O_{inner}$	3.085	VT	2.259	VM1	11.710	<M2-(O-Cl)>	2.067
ΔK	0.115	σ^2	1.00145	ψ_{M1}	58.68	VM2	11.600
		λ	6.6672	λ	1.0104	ψ_{M2}	58.56
Cl-O4	0.509 (2)	$T\text{-}O_{sheet\ thick.}$	2.228	σ^2	33.141	λ	1.0097
Cl-K	3.520(6)	$T\text{-}O_{dim.\ misfit}$	0.404	$O_{sheet\ thick.}$	2.156	σ^2	31.9282

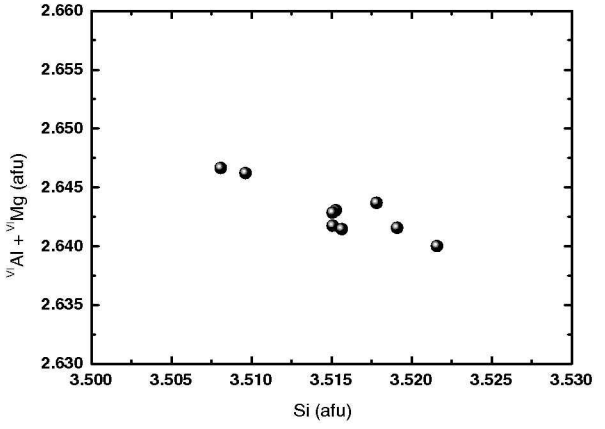

FIGURE 2. Correlation between silica and octahedral Al + Mg in apfu for the analyzed Cl-bearing, Si-rich mica.

$K_{1.01}(Mg_{2.45}Al_{0.19}\square_{0.35})_{\Sigma=3}(Si_{3.52}Al_{0.48})_{\Sigma=4}O_{10}[(OH,O)_{1.66}Cl_{0.34}]_{\Sigma=2}$, where the (OH,O^{2-}) content is calculated by difference, considering a partial dehydrogenation as suggested by the chemical analysis. In contrast to normal phlogopite (Si/Al = 3/1 with no vacancies on the octahedral sites), the present sample shows Si/Al = 3.52/0.48 and octahedral vacancies of 0.35 apfu. The Si content shows a negative correlation with the cations (Al + Mg) occupying the octahedral sites (Fig. 2) thus suggesting the coupled substitution.

The Cl-bearing, Si-rich mica has the phlogopite structure with a stacking polytype 1*M* (Fig. 3). The unit-cell parameters are given in Table 1. The T site is occupied by Si and Al. The site volume is 2.259 Å^3. The mean bond distance, 1.640 Å, is slightly shorter than that observed in a "normal" phlogopite (Brigatti and Guggenheim 2002) but very close to the value of 1.638 Å measured by Toraya et al. (1978) for the F-bearing mica $KMg_{2.75}(Si_{3.5}Al_{0.5})O_{10}F_2$.

The octahedral M1 and M2 sites are mainly occupied by Mg and minor Al. Good agreement is found between the total occupancies/vacancies measured with XRD and EPMA (Table 6). Concentration of vacancies in the M1 site is 15%, while the M2 site contains 6.5% vacancies. The M1 site volume is 11.710 Å^3. The mean bond distance of the M1 site is 2.074 Å if the Cl substitution at O4 is taken into account, while the M1-Cl bond distance is 2.319 Å. The M2 site volume is 11.600 Å^3 and the mean bond distance is 2.067 Å with the Cl substitution, where the M2-Cl distance is 2.337 Å. Flattening angles Ψ for M1 and M2, 58.68 and 58.56°, respectively, suggest a homo-octahedral character of this mica. The octahedral sheet thickness, 2.156 Å, is comparable with natural phlogopites (Brigatti and Guggenheim 2002).

The A site is completely occupied by potassium. The longest mean distance is 3.203(3) Å and the shortest is 3.085(2) Å, with a $\Delta_{K\text{-}O}$ equal to 0.115 Å. The distance of K to Cl is 3.520(6) Å.

As mentioned above, the O4 site is not fully occupied by oxygen. In fact, a peak in the Fourier difference map was found at 0.509 Å from the O4 position, where Cl was positioned. The refined occupancy of Cl (0.3932 apfu) is in good agreement with the microprobe data (Table 6). The tetrahedral rotation angle α, defined as the difference between 120° and the Φ angles formed by the basal O-O edges of adjacent tetrahedra (Toraya 1981) is 2.58°.

DISCUSSION

Formation of Cl-bearing, Si-rich micas: crystal chemical aspects

Among the substituents for OH (F, O^{2-}, Cl), the incorporation of large amounts of Cl in natural and synthetic micas is very uncommon (e.g., Volfinger and Pascal 1989; Zhu and Sverjensky 1991). Unlike fluorine analogues, pure synthetic Cl-bearing end-members for dioctahedral or trioctahedral micas are unknown. As suggested by Volfinger et al. (1985) the incorporation of chlorine is limited by pure geometric factors, i.e., the large ionic radius of

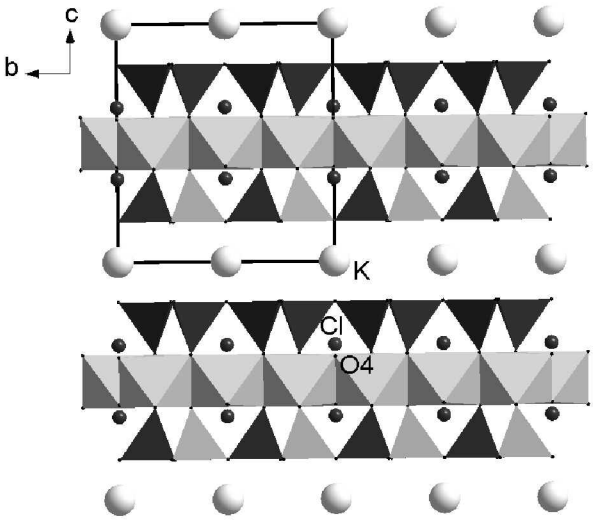

FIGURE 3. (100) projection of the Cl-bearing, Si-rich mica structure. Split position of the Cl atom is indicated.

this ion. These authors calculated the theoretical coordinates for chlorine (*x*/*a* 0.118 *y*/*b* 0 *z*/*c* 0.356) starting from the coordinates of OH and using the difference between the ionic radii. These values are in excellent agreement with the coordinates found in the present refinement, i.e., *x*/*a* 0.1178 *y*/*b* 0 *z*/*c* 0.3496 (Fig. 3). Using the ionic radius for Cl in tetrahedral coordination (1.78 Å), Volfinger et al. (1985) also calculated the theoretical Cl-O distances: 3.13 Å for Cl-O1 and Cl-O2 and 3.08 Å for Cl-O3. These values suggest that incorporation of Cl into the mica structure greatly deforms the local environment. In the present mica, we found Cl-O distances slightly higher than those calculated by Volfinger et al. (1985).

To understand the reason for incorporation of large amount of Cl in the Si-rich mica, we first should compare its structural features with those of micas that easily accommodate chlorine. For example, the strong affinity of Cl for Fe-rich micas (annite) is well known both from experimental studies and natural assemblages (e.g., Volfinger et al. 1985; Leelanandam 1969; Munoz and Swenson 1981; Léger et al. 1996). Indeed, the large ionic radius of Fe^{2+} in the annite structure expands the octahedral layer. Therefore, to account for the misfit between the octahedral and tetrahedral layers, the tetrahedral rotation angle (α) decreases: 1–3° in annite in comparison to 6–10° in phlogopite (Brigatti and Guggenheim 2002) (Fig. 4). Thus, the tetrahedral rotation angle α seems to control the entering of Cl into the mica structure, and micas with low α angle would contain more chlorine.

The *b* lattice dimension of ideal sheets consisting of hexagonal rings is 9.15 Å for the tetrahedral sheet of Si_4, 9.34 Å for (Si_3Al), whereas *b* is 9.36 Å for $Mg(OH)_3$ and 8.64 Å for $Al(OH)_2$ octahedral sheets, respectively. To adjust this lateral misfit of sheets in the stacking sequence of micas, a distortion of the hexagonal basal O atoms ring of the tetrahedral sheet is required. If the basal ring is hexagonal and α is zero, the A site cavity is of maximal size. With increasing α, the ring becomes progressively more ditrigonal and the A site cavity decreases. The reduction of α can be achieved through two mechanisms: (1) incorporation of small cations into the tetrahedral site, which

TABLE 6. Total occupancies/vacancies measured with XRD and EPMA

	XRD	EMPA
A site	2.000(1)	2.012(2)
T site		
Si	7	7.032(10)
Al	1	0.968(12)
M1 site		
Mg	1.7024(9)	
vacancy	0.2976	
M2 site		
Mg	3.7416(13)	
vacancy	0.2584	
$Mg_{M1}+Mg_{M2}$	5.4440	5.285(6)
O4	1.6068(15)	
Cl	0.3932(15)	0.337(5)

Notes: Vacancies in the M1 and M2 sites are calculated from difference to 1, respectively. The occupancies of Si and Al in T site were fixed according to the EMPA values. Estimated standard deviations refer to the last digit.

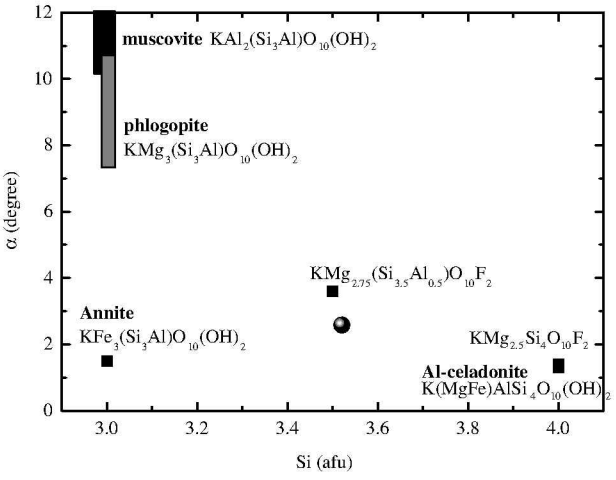

FIGURE 4. Tetrahedral rotation angle α plotted against silica content. See text for discussion. Ball = Cl-bearing, Si-rich mica; full square = micas end-members.

results in higher Si/Al ratio; (2) incorporation of large cations into the octahedral sites by increasing the annite component in biotite (responsible for the affinity of Cl for Fe-rich biotites). The first mechanism is available for the Si-rich mica. Figure 5 shows the coupled heterovalent substitutions, which link di- and tri-octahedral micas: The 3Mg = 2Al vector links phlogopite to muscovite, the Si + ^{VI}Al + □ = ^{IV}Al + 2Mg vector phlogopite to Al-celadonite, and Si + □ = ^{IV}Al + 0.5Mg phlogopite to $KMg_{2.5}Si_4O_{10}(OH)_2$ mica (Seifert and Schreyer 1971). All these substitutions need the presence of octahedral vacancies, increasing from ~17% in phlogopite-$KMg_{2.5}Si_4O_{10}(OH)_2$ mica to ~33% in the other two substitutions. Our mica clearly shows a lower *b* value than phlogopite (Fig. 6), which is consistent with the decrease of this value from phlogopite (~9.22 Å) to Al-celadonite (~9.05 Å) caused by the coupled substitution Si + ^{VI}Al + □ = ^{IV}Al + 2Mg. Along the above vectors, α varies from 6–10° in phlogopite (Brigatti and Guggenheim 2002) throughout 8–11° in the muscovite-phengite series (Brigatti and Guggenheim 2002) to 1.3° in Al-celadonite (Schmidt et al. 2001). The values of 1.4 and 3.6° are found in synthetic $KMg_{2.5}Si_4O_{10}F_2$ (Toraya et al. 1976) and $KMg_{2.75}(Si_{3.5}Al_{0.5})O_{10}F_2$ (Toraya et al. 1978), respectively. Our synthetic Cl-bearing, Si-rich mica shows a combination of these vectors: Si increases to 3.5 apfu and Mg decreases to 2.45 apfu with consequent 21% of octahedral vacancies. The vector

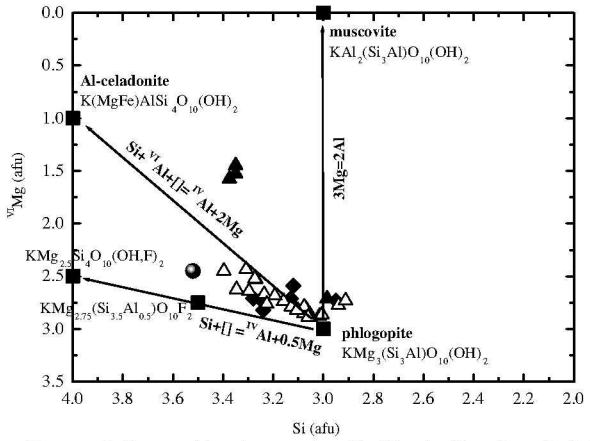

FIGURE 5. Compositional space described by the Si and octahedral Mg content of micas. See text for discussion. Full square = micas end-members. Ball = Si and Cl-rich mica. Triangle = Izraeli et al. (2004); Diamond = Harlov and Melzer (2002); empty triangle = Foley et al. (1986).

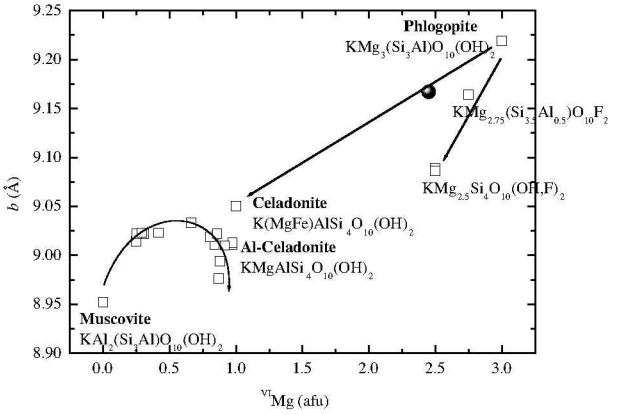

FIGURE 6. The b lattice parameter plotted against octahedral Mg content. Data on the muscovite-celadonite join (Schmidt et al. 2001) are reported for comparison. See text for discussion.

that describes the heterovalent substitution in the Cl-bearing, Si-rich mica is $0.52Si + 0.2^{VI}Al + 0.35\square = 0.52^{IV}Al + 0.55Mg$. It is evident from the above values that α would greatly decrease along this vector. In fact, the studied mica has α = 2.58° (Fig. 4), and the basal oxygen ring is nearly hexagonal. This configuration, resulted from the complex heterovalent substitution involving octahedral and tetrahedral cations, is favorable to host chlorine.

Moreover the partial di-octahedral character of this Cl-bearing, Si-rich mica might be recorded by IR and NMR spectroscopy, which are sensitive to local structure environments in micas. The chemical shift associated with Si and Al in the NMR spectra of micas has different values related both with Si-Al tetrahedral substitution and di- or tri-octahedral structure (Sanz and Serratosa 1984). In the IR spectra of micas, the Si-O vibration mode near 1100 cm^{-1} is sensitive to the di- or tri-octahedral character, showing a decrease in wavenumber with celadonitic substitution (Velde 1978). In the far-IR region the torsional mode interlayer frequency ν_i is directly related to the tetrahedral sheet environment (i.e., tetrahedral rotation angle α) (Schroeder 1990): it increases in wavenumber from 87 cm^{-1} in phlogopite to 102 cm^{-1} in celadonite to 108 cm^{-1} in muscovite. Furthermore a strong correlation with the OH-F substitution has been suggested to influence the ν_i frequency, with frequency increasing with F content (Schroeder 1990). It is reasonable to suppose that the OH-Cl substitution will strongly influence this mode, too.

In phlogopite the tetrahedral rotation angle α increases with pressure, from 9.3 to 11.9° within the pressure interval 0.0001–6 GPa (Comodi et al. 2004). The difference in compressibility of the tetrahedral and octahedral sheets is balanced through the tetrahedral rotation. In fact, the mica structure tends to be destabilized when the α angle is too large since the tetrahedral and octahedral cations become closer, with a resulting increase in the electrostatic energy (Griffen 1992). As a consequence, any crystal-chemical mechanism that reduces the α rotation allows the structure to support high pressures (Comodi et al. 2004). In the Cl-bearing, Si-rich mica the low α rotation is achieved through the Al-celadonite component of the phlogopite, enhancing its stability at high pressure.

Data by Harlov and Melzer (2002) indicate that micas produced at 2 GPa are richer in Cl than those produced at 1 GPa, and that high-pressure micas are richer in Si. Therefore, the apparent increase of the Cl content in micas could be a result of the increase of the "Si-rich mica" content in the solid solution with pressure.

Formation of Cl-bearing, Si-rich micas: petrological aspects

Formation of the Si-rich end-members in the phlogopite solid solution can be described by the following equilibrium:

$$Phl + [21/5SiO_2 + 2/5K_2O + 4/5H_2O] = Al\text{-}Cel + 4/5KMg_{2.5}Si_4O_{10}(OH)_2,$$

which depends on SiO_2, K_2O, and H_2O activity in the mineral-forming medium (fluid or melt). According to this equilibrium, silica activity is, probably, the most important factor in the formation of Si-enriched phlogopite. Available experimental data confirm this suggestion. For example, in the run products of Foley et al. (1986) the most Si-rich micas (6.5–6.8 apfu) are found in association with quartz, while micas with 5.8–6.2 apfu of Si coexist with kalsilite or forsterite. Micas with intermediate Si content (6.4–6.6 apfu) are associated with sanidine. Micas from the system $CaMgSi_2O_6$-$NaAlSi_2O_6$-KCl at 4 GPa (1252, 1249, and 1299; Safonov, unpublished data) coexist with sanidine and silica-rich melt (63–65 wt% of SiO_2), while Cl-bearing phlogopite in the run products in the system $Mg_3Al_2Si_3O_{12}$-$CaCO_3$-Na_2CO_3-KCl at 5 GPa (Safonov, unpublished data) is associated with spinel, forsterite, and silica-poor carbonate-silicate melt (35–38 wt% of SiO_2).

If the silica activity is low, high potassium activity could be an additional factor controlling the stability of Si-enriched phlogopite. In fact, such micas form in equilibrium with highly potassic silicate melts (e.g., Foley et al. 1986; Safonov et al. 2005). Si-rich micas in the run products 1252, 1249, and 1299, synthesized in the system $CaMgSi_2O_6$-$NaAlSi_2O_6$-KCl, coexist with silicate melts whose K_2O content is 12–16 wt%, while the concentration of K_2O in the melt in the run 1132 [system $CaMgSi_2O_6$-$KAlSi_3O_8$-

$Mg(OH)_2$-KCl; Safonov et al. 2005] reaches 23 wt%. The lower a_{SiO_2}, the higher a_{K_2O} would be in order to stabilize Si-enriched phlogopite. This conclusion is fully supported by the observation of such micas in the phlogopite-alkali chloride systems (Melzer and Wunder 2001; Harlov and Melzer 2002).

Natural data prove that Si-rich micas are indicators of high alkali activity. Seifert and Schreyer (1971) first addressed occurrences of "high-silica phlogopites" in specific rocks like carbonatites, kimberlites, and alkalic basic rocks. Regarding alkalic rocks, like madupites, wolgidites, and jumillites, Seifert and Schreyer (1971) pointed out that the main factor influencing formation of Al-deficient, Si-rich micas is the high alkalinity, since alkalis binds alumina to form aluminosilicates. Robert and Maury (1979) described tetrasilicic potassium mica in comendite from the Mont-Dore massif, while Velde (1979) found similar mica in melilitic rocks.

Most of the above micas contain fluorine. The highest content, 4.4 wt%, is reported by Robert and Maury (1979). However, Cl-rich, Si-enriched phlogopite has never been observed in low-pressure natural assemblages. Data by Izraeli et al. (2004) and Klein-BenDavid et al. (2006) expand occurrence of Si-rich micas for the diamond-related pressures and Cl-rich environments. Formation of these micas is also related to the high activity of potassium in the coexisting liquids. Differences in the Si content in the micas from diamonds of the Koffiefontein pipe (Izraeli et al. 2004) and the Diavik mine (Klein-BenDavid et al. 2006) are explainable in terms of the above equilibrium. Higher concentration of SiO_2 (27 wt%) in the carbonate-silicate melt coexisting with the mica in the Diavik diamonds, probably, is responsible for higher Si content in the mica. High potassium content in this melt (22 wt% of K_2O) is the determining factor for formation of such mica, as well. In contrast, much lower SiO_2 content (3–7 wt%) in the chloride-carbonate brine coexisting with the mica in the Koffiefontein diamonds would prevent from high Si content in the mica. However, high potassium content (26–36 wt% of K_2O) still assists in the formation of the Al-celadonite component in the mica solid solution.

It is evident from the experimental data of Harlov and Melzer (2002) and our present experiments (see also Safonov et al. 2005) that, despite the assistance of the "Si-mica" component for incorporation of Cl in the phlogopite, high Cl content in this mineral can be produced only in equilibrium with highly chloride-rich media (brines, chloride melts). It means that the partitioning coefficient of Cl between mica and melts is very low. This conclusion explains why the Si-rich mica inclusions in the Diavik mine are chlorine-poor (Klein-BenDavid et al. 2006). The Cl content in the coexisting carbonate-silicate melt (1.8 wt%) is not enough to allow the entrance of chlorine into the mica. In contrast, chlorine-rich brine (up to 42 wt% Cl) is responsible for crystallization of Cl-rich Si-mica within the inclusions in the Koffiefontain diamonds (Izraeli et al. 2004).

Besides data by Izraeli et al. (2004) and Klein-BenDavid et al. (2006), there are few reports of Si-enriched phlogopites in diamonds (Guthrie et al. 1991). Walmsley and Lang (1992) measured the cation ratio in the mica from the Zairean diamond: Mg 0.86, A1 0.92, Si 4.74, K 1.0, Ti 0.3, and Fe 0.86. They also noted minor Cl content in this mica. These authors attributed an extremely high Si content to a presence of some Si-rich phase coexisting with the mica. Nevertheless, the above cation ratio allows rough determination of the Si content, which is enough to compensate Mg, Fe, Al, Ti, and K at 22 negative charges (O + OH + Cl). The calculation shows that the Si content in this mica could reach 6.95 apfu. At this Si content, a total concentration of octahedral cations could be 4.83 apfu, with 1.17 apfu of vacancies. These values are in a good agreement with the phlogopite-Al-celadonite vector (Fig. 6). High Al-celadonite content and the presence of minor Cl in the mica resembles these characteristics of mica inclusions described by Klein-BenDavid et al. (2006) in the Canadian diamonds. These features imply that the mica from the Zairean diamond could be in equilibrium with highly potassic Cl-bearing carbonate-silicate liquid. In fact, such kind of liquid inclusions is found in the Zairean diamonds (e.g., Navon et al. 1988).

Shatsky et al. (2008) described inclusions of Si-enriched mica in diamonds extracted from the eclogite xenolith from the Udachnaya kimberlite pipe (Yakutia). Silicon content in this mica varies from 6.3 to 6.6 apfu, while chlorine content is low (D. Zedgenizov, pers. comm.). The xenolith itself contains normal phlogopite (5.9–6.0 apfu of Si). It shows that both types of micas in this xenolith were formed at very different conditions. Taking into account the composition of the mica inclusions in diamond, we can conclude that they were precipitated along with diamond from alkalic carbonate-silicate melt interacting with the phlogopite-bearing eclogite. Indeed, Shatsky et al. (2005) deduced an origin for diamonds in this eclogite via interaction with some external fluid, while Zedgenizov et al. (2007) observed ubiquitous alkalic carbonate-silicate melt inclusions in the Udachnaya diamonds.

Thus, the crystal chemistry and composition of Si-rich micas are very sensitive to potassium activity in the upper mantle. Since their crystal chemical characteristics are suitable for accumulation of chlorine, Si-rich micas are indicators of chlorine activity, as well. Taking into account the published data on relics of alkaline chlorine-rich liquids in diamonds (see Navon et al. 2003 and Safonov et al. 2007), as well as new data on the role of mantle-originated chlorine in the genesis of kimberlitic magmas (e.g., Kamenetsky et al. 2004; Maas et al. 2005; Kamenetsky et al. 2007), our present data provide a new mineral indicator of such unique liquids in the Earth's upper mantle.

ACKNOWLEDGMENTS

We thank Alexei N. Nekrasov and Konstantin V. Van (IEM RAS) for providing facilities for electron microprobe analyses. We are grateful to N.V. Sobolev and an anonymous reviewer, as well as to the Associate Editor P. Schroeder for suggestions, which greatly improve the paper. The study is supported by the Russian Foundation for Basic Research (projects 07-05-00499 to O.G.S., 06-05-64196 to L.L.P., 05-05-64101 to Y.A.L.), the RF President's Grant for Young Scientists (Project MD-130.2008.5 to O.G.S.), the RF President's Leading Scientific Schools Program (grant 1949.2008.5 to L.L.P.), the RAS Project P-9-3 for Material Study at Extreme Conditions, Russian Science Support Foundation, and by the Italian MURST grant to P.C. (COFIN 2005–2007, "Ruolo delle fasi contenenti volatili nei processi di interazione crosta-mantello: evidenze dalla campagna e dal laboratorio").

REFERENCES CITED

Brigatti, M.F. and Guggenheim, S. (2002) Mica crystal chemistry and the influence of pressure, temperature, and solid solution on atomistic models. In A. Mottana, F.P. Sassi, J.B. Thompson, and S. Guggenheim, Eds., Micas: Crystal Chemistry and Metamorphic Petrology, 46, p. 1–97. Reviews in Mineralogy and Geochemistry, Mineralogical Society of America, Chantilly, Virginia.

Bulanova, G.P., Barashkov, Y.P., Tal'nikova, S.B., and Smelova, G.B. (1993) Natural diamond—genetic aspect. Nauka Press, Novosibirsk (in Russian).

Comodi, P., Fumagalli, P., Montagnoli, M., and Zanazzi, P.F. (2004) A single-crystal study on the pressure behavior of phlogopite and petrological implication. American Mineralogist, 89, 647–653.

Domanik, K.J. and Holloway, J.R. (2000) Experimental synthesis and phase relations of phengitic muscovite from 6.5 to 11 GPa in a calcareous metapelite from the Dabie Mountains, China. Lithos, 52, 51–77.

Foley, S.F., Taylor, W.R., and Green, D.H. (1986) The effect of fluorine on phase relationships in the system $KAlSiO_4$-Mg_2SiO_4-SiO_2 at 28 kbar and the solution mechanism of fluorine in silicate melts. Contributions to Mineralogy and Petrology, 93, 46–55.

Franz, G. and Althaus, E. (1974) Synthesis and thermal stability of 2.5-octahedral sodium mica, $NaMg_{2.5}[Si_4O_{10}](OH)_2$. Contributions to Mineralogy and Petrology, 46, 227–232.

Giardini, A.A., Hurst, V.J., Melton, C.E., and Stormer, J.C. (1974) Biotite as a primary inclusion in diamond: Its nature and significance. American Mineralogist, 59, 783–789.

Griffen, D.T. (1992) Silicate Crystal Chemistry. Oxford University Press, New York.

Gurney, J.J., Harris, J.W., and Rickard, R.S. (1979) Silicate and oxide inclusions in diamonds from the Finsch kimberlite pipe. In F.R. Boyd and H.O.A. Meyer, Eds., Kimberlites, Diatremes and Diamonds: Their Geology, Petrology, and Geochemistry, p. 1–15. American Geophysical Union, Washington.

Guthrie, G.D., Veblen, D.R., Navon, O., and Rossman, G.R. (1991) Submicrometer fluid inclusions in turbid-diamond coats. Earth and Planetary Science Letters, 105, 1–12.

Harlov, D.E. and Melzer, S. (2002) Experimental partitioning of Rb and K between phlogopite and concentrated (K, Rb)Cl brine: Implication for the role of concentrated KCl brines in the depletion of Rb in phlogopite and the stability of phlogopite during charnockite genesis. Lithos, 64, 15–28.

Harlow, G.E. (2002) Diopside + F-rich phlogopite at high *P* and *T*: Systematics, crystal chemistry and stability of $KMgF_3$, clinohumite, and chondrodite. Geological Materials Research, 4, 1–28.

Ibers, J.A. and Hamilton, W.C. (1974) International Tables for X-ray Crystallography, 4, p. 99–101. Kinoch, Birmingham, U.K.

Izraeli, E.S., Harris, J.W., and Navon, O. (2004) Fluid and mineral inclusions in cloudy diamonds from Koffiefontein, South Africa. Geochimica et Cosmochimica Acta, 68, 2561–2575.

Kamenetsky, M.B., Sobolev, A.V., Kamenetsky, V.S., Maas, R., Danyushevsky, L.V., Thomas, R., Pokhilenko, N.P., and Sobolev, N.V. (2004) Kimberlite melts rich in alkali chlorides and carbonates: A potent metasomatic agent in the mantle. Geology, 32, 845–848.

Kamenetsky, V.S., Kamenetsky, M.B., Sharygin, V.V., Faure, K., and Golovin, A.V. (2007) Chloride and carbonate immiscible liquids at the closure of kimberlite magma evolution (Udachnaya-East kimberlite, Siberia). Chemical Geology, 237, 384–400.

Klein-BenDavid, O., Wirth, R., and Navon, O. (2006) TEM imaging and analysis of microinclusions in diamonds: A close look at diamond-bearing fluids. American Mineralogist, 91, 353–356.

Leelanandam, C. (1969) Electron microprobe analyses of chlorine in hornblendes and biotites from the charnockitic rocks of Kondapalli, India. Mineralogical Magazine, 37, 362–365.

Léger, A., Rebbert, C., and Webster, J. (1996) Cl-rich biotite and amphibole from Black Rock Forest, Cornwall, New York. American Mineralogist, 81, 495–504.

Leost, I., Stachel, T., Brey, G.P., Harris, J.W., and Ryabchikov, I.D. (2003) Diamond formation and source carbonation: Mineral associations in diamonds from Namibia. Contributions to Mineralogy and Petrology, 145, 15–24.

Maas, R., Kamenetsky, M.B., Sobolev, A.V., Kamenetsky, V.S., and Sobolev, N.V. (2005) Sr, Nd, and Pb isotope evidence for a mantle origin of alkali chlorides and carbonates in the Udachnaya kimberlite, Siberia. Geology, 33, 549–552.

Melzer, S. and Wunder, B. (2001) K-Rb-Cs partitioning between phlogopite and fluid: Experiments and consequences for the LILE signatures of island arc basalts. Lithos, 59, 69–90.

Munoz, J.L. and Swenson, A. (1981) Chloride-hydroxyl exchange in biotite and estimation of relative HCl/HF activities in hydrothermal fluids. Economic Geology, 76, 2212–2221.

Navon, O., Hutcheon, I.D., Rossman, G.R., and Wasserburg, G.L. (1988) Mantle derived fluids in diamond micro-inclusions. Nature, 335, 784–789.

Navon, O., Izraeli, E.S., and Klein-BenDavid, O. (2003) Fluid inclusions in diamonds—the carbonatitic connection. 8th International Kimberlitic Conference, Victoria, Canada, Extended Abstracts.

Oberti, R., Ungaretti, L., Tlili, A., Smith, D.C., and Robert, J.L. (1993) The crystal structure of preiswerkite. American Mineralogy, 78, 1290–1298.

Prinz, M., Manson, D.V., Hlava, P.F., and Keil, K. (1975) Inclusions in diamonds: Garnet lherzolite and eclogite assemblages. Physics and Chemistry of Earth, 9, 797–815.

Robert, J.L. and Kodama, H. (1988) Generalization of the correlations between hydroxyl-tretching wavenumbers and composition of micas in the system K_2O-MgO-Al_2O_3-SiO_2-H_2O: A single model from trioctahedral and dioctahedral micas. American Journal of Sciences, 288A, 96–212.

Robert, J.L. and Maury, R.C. (1979) Natural occurrence of a (Fe,Mn,Mg) tetrasilicic potassium mica. Contributions to Mineralogy and Petrology, 68, 117–123.

Safonov, O.G., Litvin, Y.A., Perchuk, L.L., Bindi, L., and Menchetti, L. (2003) Phase relations of potassium-bearing clinopyroxene in the system $CaMgSi_2O_6$-$KAlSi_2O_6$ at 7 GPa. Contributions to Mineralogy and Petrology, 146, 120–133.

Safonov, O.G., Levykina, O.A., Perchuk, L.L., and Litvin, Y.A. (2005) Liquid immiscibility and phase equilibria in chloride-aluminosilicate melts at 4–7 GPa. Doklady Earth Science, 400, 119–123.

Safonov, O.G., Perchuk, L.L., and Litvin, Y.A. (2007) Melting relations in the chloride-carbonate-silicate systems at high-pressure and the model for formation of alkalic diamond-forming liquids in the upper mantle. Earth and Planetary Science Letters, 253, 112–128.

Sanz, J. and Serratosa, J.M. (1984) ^{29}Si and ^{27}Al high resolution MAS-NMR spectra of phyllosilicates. Journal of the American Chemical Society, 106, 4790–4793.

Schroeder, P. (1990) Far infrared, X-ray powder diffraction, and chemical investigation of postassium micas. American Mineralogist, 75, 983–991.

Schmidt, M.W. and Poli, S. (1998) Experimentally based water budgets for dehydrating slabs and consequences for arc magma generation. Earth and Planetary Science Letters, 163, 361–379.

Schmidt, M.W., Dugnani, M., and Artioli, G. (2001) Synthesis and characterization of white micas in the join muscovite-aluminoceladonite. American Mineralogist, 86, 555–565.

Seifert, F. (1968) X-ray powder data for Mg-Al-celadonite (leucophyllite) from Barcza, Poland. Contributions to Mineralogy and Petrology, 19, 93–96.

Seifert, F. and Schreyer, W. (1965) Synthesis of a new mica $KMg_{2.5}(Si_4O_{10})(OH)_2$. American Mineralogist, 50, 1114–1118.

——— (1971) Synthesis and stability of micas in the system K_2O-MgO-SiO_2-H_2O and their relation to phlogopite. Contributions to Mineralogy and Petrology, 30, 196–215.

Shatsky, V.S., Zedgenizov, D.A., Ragozin, A.L., Mityukhin, S.I., and Sobolev, N.V. (2005) Evidence for metasomatic formation of diamond in the eclogite xenolith from the Udachnaya kimberlite pipe (Yakutia). Doklady Earth Sciences, 402, 587–590.

Shatsky, V.S., Ragozin, A.L., and Zedgenizov, D.A. (2008) Evidence for mantle modification in xenolith of diamond-bearing eclogite from the Udachnaya kimberlite pipe. Lithos, in press.

Sheldrick, G.M. (1996) SADABS. Program for empirical absorption correction of area detector data. Institut für Anorganische Chemie, University of Göttingen, Germany.

——— (1997) SHELXL-97. Program for crystal structure refinement. University of Göttingen, Germany.

Sobolev, N.V., Kaminsky, F.V., Griffin, W.L., Yefimova, E.S., Win, T.T., Ryan, C.G., and Botkunov, A.I. (1997) Mineral inclusions in diamonds from the Sputnik kimberlite pipe, Yakutia. Lithos, 39, 135–157.

Sobolev, N.V., Yefimova, E.S., Channer, D.M.DeR., Anderson, P.F.N., and Barron, K.M. (1998) Unusual upper mantle beneath Guaniamo, Guyana Shield, Venezuela: Evidence from diamond inclusions. Geology, 26, 971–974.

Toraya, H. (1981) Distortions of octahedral and octahedral sheets in 1*M* micas and the relation to their stability. Zeitschrift für Kristallographie, 157, 173–190.

Toraya, H., Iwai, S., Marumo, F., Daimon, M., and Kondo, R. (1976) The crystal structure of tetrasilic potassium fluor mica, $KMg_{2.5}(Si_4O_{10})F_2$. Zeitschrift für Kristallographie, 144, 42–52.

——— (1978) The crystal structure of tetrasilic potassium fluor mica, $KMg_{2.5}(Si_4O_{10})F_2$. Zeitschrift für Kristallographie, 144, 42–52.

Trønnes, R.G. (2002) Stability range and decomposition of potassic richterite and phlogopite end-members at 5–15 GPa. Mineralogy and Petrology, 74, 129–148.

Velde, B. (1978) Infrared spectra of synthetic micas in the series muscovite-MgAl celadonite. American Mineralogist, 63, 343–349.

Velde, D. (1979) Trioctahedral micas in melilite-bearing eruptive rocks. Carnegie Institute of Washington Yearbook, 78, 468–475.

Volfinger, M. and Pascal, M.L. (1989) Partitioning of chlorine between muscovite and HCl-buffered solutions from 400 to 600 °C at 2 kbar. European Journal of Mineralogy, 1, 791–800.

Volfinger, M., Robert, J.L., Vielzeuf, D., and Neiva, A.M.R. (1985) Structural control of the chlorine content of OH-bearing silicates (micas and amphiboles). Geochimica et Cosmochimica Acta, 49, 37–48.

Walmsley, J.C. and Lang, A.R. (1992) Oriented biotite inclusions in diamond coat. Mineralogical Magazine, 56, 108–111.

Yoder, H.S. and Kushiro, I. (1969) Melting of hydrous phase: Phlogopite. American Journal of Sciences, 267A, 558–582.

Zedgenizov, D.A., Rege, S., Griffin, W.L., Kagi, H., and Shatsky, V.S. (2007) Composition of trapped fluids in cuboid fibrous diamonds from the Udachnaya kimberlite: LAM-ICPMS analysis. Chemical Geology, 240, 151–162.

Zhu, C. and Sverjensky, D.A. (1991) Partitioning of F-Cl-OH between minerals and hydrothermal fluids. Geochimica et Cosmochimica Acta, 55. 1837–1858.

MANUSCRIPT RECEIVED SEPTEMBER 24, 2007
MANUSCRIPT ACCEPTED JANUARY 30, 2008
MANUSCRIPT HANDLED BY PAUL SCHROEDER